

CURRENT DESIGN STATUS OF TPS 3 GEV BOOSTER SYNCHROTRON

H. C. Chao*, H. P. Chang, H. J. Tsai, P. J. Chou, G. H. Luo and C. C. Kuo
NSRRC, Hsinchu 30076, Taiwan, R. O. C.

Abstract

The design work of the concentric booster for Taiwan Photon Source (TPS) has been well in progress. The circumference is 496.8 m. It consists of modified FODO cells with defocusing quadrupole and sextupole fields built in bending magnets, and combined function focusing quadrupoles with embedded focusing sextupole. The emittance is about 10 nm-rad at 3 GeV. Several modifications on the structure were made to improve the beam dynamics behaviors. Good dynamic aperture and nonlinear behavior as well as good tunability are shown. The efficient closed orbit correction scheme is presented. The repetition rate is 3 Hz, and the eddy current effect is also discussed.

INTRODUCTION

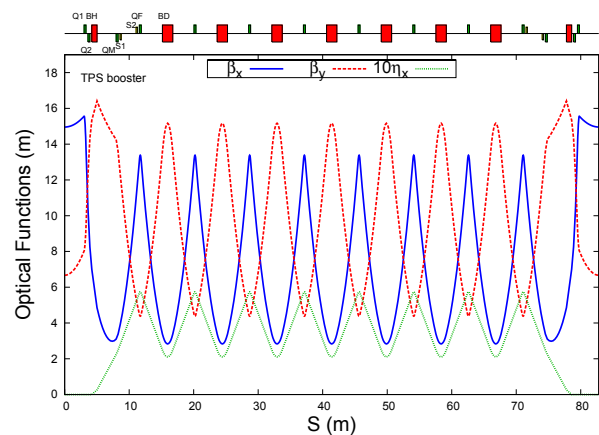
The TPS storage ring [1], with 518.4 m long and a six-fold symmetry, consists of 24 periods of DBA cells. It has six 12 m long straight sections and eighteen 7 m long standard straight sections. The TPS concentric booster, with 496.8 m in circumference, is designed to share the same tunnel with the storage ring due to the limited available space on the existing site. The booster will accommodate the 150 MeV beam from LINAC, raise the beam energy up to 3 GeV and then get the beam extracted. The booster also has six-fold symmetry geometry to fit the shape of storage ring outside. There are six 6.02 m straight sections which are non-dispersive. The basic parameters of the booster are listed in Table 1.

Table 1: Booster Ring Parameters

Circumference	496.8 m
Straight section length	6.02 m
Injection energy	150 MeV
Extraction energy	3.0 GeV
Harmonic number	828
RF frequency	499.654 MHz
Betatron tune	14.369/9.405
Natural chromaticity	-16.86/-13.29
Damping partition	1.82/1.00/1.18
Energy Spread at 3 GeV	0.09553 %
Natural emittance at 3 GeV	10.32 nm-rad
Damping time at 3 GeV	9.34/16.96/14.32 msec
Dipole field at 3 GeV	0.82 T
Energy loss per turn at 3 GeV	586 KeV
Ramping repetition rate	3 Hz

Each superperiod contains 7 modified FODO cells and two dispersion suppressors. The modified FODO cells consists of one 1.6 m bending magnet combined

with defocusing quadrupole and sextupole fields and one combined function focusing quadrupoles with embedded focusing sextupole. The embedded sextupole fields are designed to make the chromaticities to (+1, +1). The dispersion suppressor consists of one separated function quadrupole and one combined function dipole, with the same iron lamination but half the length as the bending magnets of the FODO cell. Pairs of extra sextupoles are put in dispersion suppressor section to adjust the chromaticities dynamically. Outside the dispersion suppressors there are two families of separated function quadrupoles for matching the beta functions in straight sections. The optical functions are shown in Fig. 1.



near the defocusing elements. The locations of the BPMs and correctors are indicated in the Fig. 2. The strengths of corrector can be easily obtained by the SVD method. Some statistics of BPM records of 50 random machines before and after orbit correction are listed in Table 2. The maximum corrector strength used is less than 0.3 mrad and the average rms value is about 0.07 mrad.



Figure 2: The locations of BPMs and correctors in one superperiod. The horizontal correctors are indicated in blue arrows and the vertical correctors in pink arrows. The BPMs are indicated in short black lines.

Table 2: BPM Statistics Before and After Orbit Correction

For all BPM Readings	Before Correction		After Correction	
	Horizontal	Vertical	Horizontal	Vertical
max abs (mm)	10.4649	8.0664	0.5515	0.4384
avg rms (mm)	2.8538	1.5394	0.0918	0.0936

NONLINEAR BEHAVIORS AND DYNAMIC APERTURE

Particle tracking codes like TRACY2 and OPA are used to study the nonlinear behavior and dynamic aperture simulation. Particle is considered stable if it survives after 1024 turns. The tune shifts with amplitude and tune shifts with energy of the bare lattice are depicted in Fig. 3. One can see that the variations of tunes due to different amplitudes and energies are quite small.

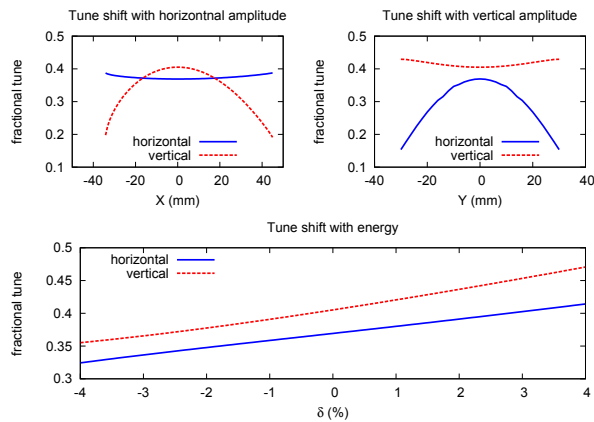


Figure 3: Tune shifts with amplitude and energy.

The phase space diagrams of the bare lattice for the horizontal and vertical planes are shown in Fig. 4. The tracking point is at the center of straights, where β_x is 15.0 and β_y is 6.7.

The systematic multipole field errors of the booster magnets are given in Table 3. The numbers are estimated by a fitting technique. The designed good field region is

Light Sources and FELs

A05 - Synchrotron Radiation Facilities

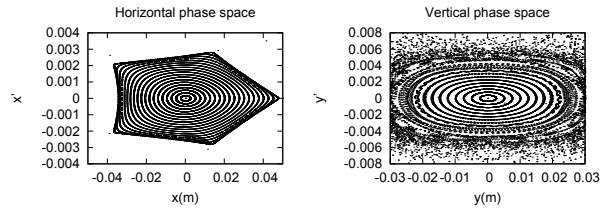


Figure 4: Phase space tracking.

within ± 15 mm. With this error set, the dynamic aperture for both on and off-momentum are shown in Fig. 5.

Table 3: Typical multipole field error set. The magnetic

field can be expressed as $B_y(x) = \sum_{n=0}^{\infty} b_n x^n$.

combined function quadrupoles				
b5L/b1L	b8L/b1L	b9L/b1L	b13L/b1L	b14L/b1L
2.79E+04	1.89E+07	2.14E+11	-5.04E+18	-9.06E+19
b17L/b1L	b20L/b1L			
5.57E+24	5.53E+29			
seperated function quadrupoles				
b5L/b1L	b9L/b1L	b13L/b1L	b17L/b1L	b21L/b1L
-3.11E+03	1.59E+11	-7.04E+17	-2.63E+25	7.51E+31
combined function bending magnets				
b4L/b0L	b5L/b0L	b6L/b0L	b8L/b0L	b9L/b0L
8.38E+02	5.72E+04	-4.04E+06	-2.38E+10	-2.12E+12
b10L/b0L	b12L/b0L	b13L/b0L	b14L/b0L	
-9.25E+13	-2.50E+17	7.21E+18	1.20E+19	
sextupoles				
b8L/b2L	b14L/b2L	b20L/b2L	b26L/b2L	b32L/b2L
2.97E+07	-4.44E+18	-3.70E+28	-1.93E+39	1.58E+49

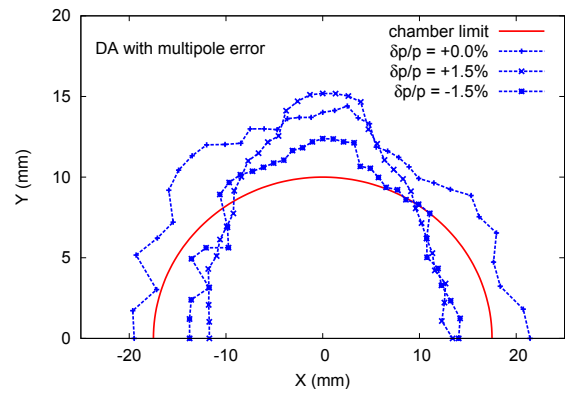


Figure 5: Dynamic aperture ($\beta_x = 15.0$, $\beta_y = 6.7$). A chamber limit of 17.5 mm \times 10 mm is also indicated.

RANGE OF TUNES AND VERTICAL EMITTANCE SCAN

High tolerance to magnet errors are demonstrated. A tune shift of $(-0.036, +0.156)$ caused by 1 % of gradient error in every combined function bending magnet can be corrected easily.

The working tunes can be adjusted by changing the strengths of the two families of quadrupoles in the sides of the straight sections. Table 4 shows different modes of working tunes and the corresponding quadrupole settings. One can see in the extreme case, the maximum quadrupole strength is less than 1.5 1/m^2 .

Table 4: Different operation modes, the quadrupole strength is defined as $K_1 = \frac{1}{B\rho} \frac{\partial B_y}{\partial x}$.

Qx	Qy	$K_1(Q1)$	$K_1(Q2)$
14.020	9.020	1.1982	-0.6829
14.020	9.480	1.3080	-0.8480
14.480	9.020	1.4134	-0.8320
14.480	9.480	1.4942	-0.9653
14.369	9.405	1.4355	-0.9086
14.380	9.280	1.4091	-0.8618

Betatron coupling arises from the rotational errors of quadrupole field and the vertical orbit deviations in sextupole field. The contour plot of the projected vertical emittance with different tune range is shown in Fig. 6. The projected emittance is obtained by the method of Edwards and Teng [2], and the invariants are calculated using the method of Chao [3].

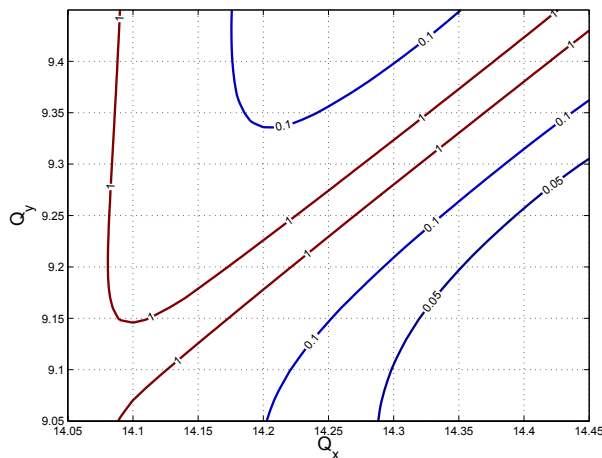


Figure 6: Contour of projected vertical emittance (nm-rad).

EDDY CURRENT EFFECT

The energy is ramped from 50 MeV to 3 GeV in a sinusoidal way during the ramping-up cycle so that the injected beam can take off on-the-fly. The 150 MeV beam from LINAC is injected at about 20 ms from the start of the ramping cycle. The largest chromaticity change when the beam exists in the booster ring is at the moment when the beam is just injected from LINAC. The effect of eddy current on the variation of the chromaticities is shown as Fig. 7. Here a model of two parallel, infinitely expanded plates is assumed for the shape of the vacuum chamber at bending magnets.

The independent sextupoles are used to compensate the chromaticity changes due to the eddy current. The dynamic aperture is still good enough even when the chromaticities are corrected to $(+5, +5)$ for this worst case.

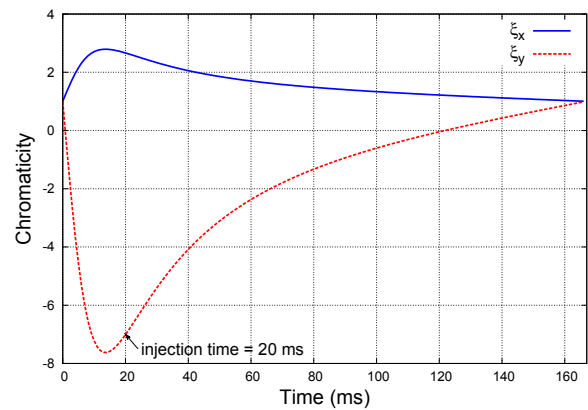


Figure 7: Eddy current effect.

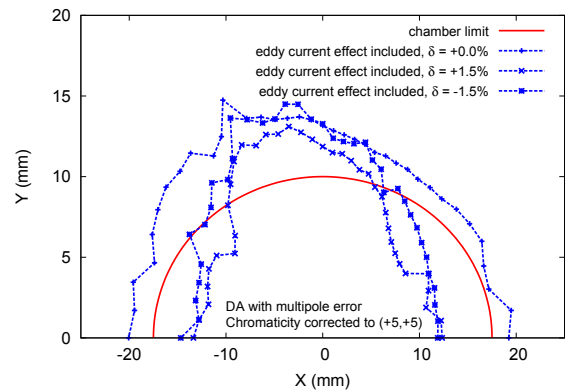


Figure 8: Dynamic aperture after correction of eddy current effect ($\beta_x = 15.0, \beta_y = 6.7$).

REFERENCES

- [1] C. C. Kuo, et al, "Progress Report of TPS Lattice Design", this proceedings.
- [2] D. A. Edwards and L. C. Teng, "Parameterization of linear coupled motion in periodic system", PAC'73, 1973
- [3] A. W. Chao, "Evaluation of beam distribution parameters in an electron storage ring", J.Appl.Phys. 50, Feb 1979, p595